ISABE-2015-20099

ANALYTICAL STUDY OF THE IMPACT OF AIRFOIL CONTOUR TOLERANCE FOR A PROPULSION LPT BLADE ON TURBINE PERFORMANCE

Hector C. Garcia
Honeywell International
Chihuahua, Chihuahua 31074, MEXICO

Paul T. Couey
Honeywell International
Phoenix, Arizona 85034, USA

Abstract

This study presents a summary of a numerical analysis of blade airfoil contour variation upon the resulting turbine stage performance parameters for a typical LPT blade. The main focus of the study is to determine how the casting airfoil contour tolerance matched to current casting process capability is impacting the blade-row aerodynamics. Using the airfoil design section definition of a typical propulsion engine LPT blade, the major turbine stage performance parameters affected by casting airfoil contour variation are calculated. First, a 2D cascade screening DOE analysis is used to identify which regions of the airfoil contour have the strongest influence on performance. Then, the worst-case airfoil shape identified by the cascade analysis is used in a 3D CFD stage analysis to determine the effect of the deviant blade contour on turbine stage performance parameters.

Nomenclature

μ	Dynamic viscosity
KE	Kinetic energy
$\Delta\overline{Vy}$	Normalized Turning
W	Mass flow
$\Delta P'/P'$	Total pressure loss
y+	y+ parameter
Cp	Heat capacity
k	Thermal conductivity
Tu	Turbulence intensity
γ	Heat capacity ratio
N	Rotational speed
M	Mach number
$\Delta h'$	Work extraction
η	Stage adiabatic efficiency
τ	Torque
θ	Temperature normalized to standard day (518.69 °R)
δ	Pressure normalized to standard day (14.696 psia)

Subscripts

corr	Corrected parameter
t	Total flow parameters
s	Static parameters
0	Stator inlet
1	Blade inlet
2	Blade exit

Abreviations

LPT	Low Pressure Turbine
DOE	Design of Experiments
CFD	Computational Fluid Dynamics
LE	Leading Edge
TE	Trailing Edge
PS	Pressure Side
SS	Suction Side
SSTE	Suction Side Trailing Edge
PSTE	Pressure Side Trailing Edge
SST	Shear Stress Transport
B2B	Blade to Blade
MBR	Multi-Blade-Row
2D	Two Dimensional
3D	Three Dimensional

Introduction

In the manufacturing processes involved in LPT blade production, the casting process is the one most directly affecting turbine aerodynamic performance. Modern turbine airfoils are often produced through investment casting and the airfoil shape greatly depends on the wax die geometry and several main process parameters.

Features like airfoil contour, airfoil twist, airfoil bow, etc, all depend on how capable the investment casting process is to match the aerodynamic design intent.

One of the challenges of turbine blade design for the manufacturing environment is to get a fair balance between design performance and manufacturability. Therefore, there are continuous efforts to evaluate casting tolerance impacts on airfoil performance.

Early work in this area was performed by Bammert and Sandstede [1,2]. They studied the influence of surface roughness and profile variation on blade-row performance with a four-stage air turbine. The airfoil contours were varied by thickening and thinning the shapes uniformly. Their measurements showed that efficiency was highly dependent on surface roughness and to a lesser extent, the profile changes.

More recently, Bunker [3] explored how manufacturing tolerances affect the cooling of turbine blades. He considered the geometric variation of both internal cooling features as well as external airfoil parameters. A simplified thermal analysis was used to show how metal temperatures were affected by tolerances.

Kolmakova et al [4], studied the variation of some nozzle geometric airfoil parameters with CFD, investigating the effect on pressure loss, mass flow rate, and exit flow angle. By varying the parameters independently, they found that the strongest contributors, in descending order of effect, were TE radius, stagger angle, airfoil chord and blade height. In a second stage of the study, the cumulative effects were analyzed with the four parameter values set to cause an increase in mass flow and decrease in profile loss coefficient. A second case with the four parameters set to cause the opposite behavior was analyzed. Kolmakova points out that because of the complex interactions between the parameters, these cases may not have represented the true extremes.

Montomoli et al [5], using a CFD analysis of a turbine stage, showed how variation in rotor tip gap and fillet modifies the tip heat loading and tip gap leakage.

The current study builds on the previous work by exploring variation of the airfoil contour shape. In the first phase, an analytical screening design of experiments (DOE) is performed on a 2D linear cascade using an actual LPT blade airfoil contour. The nominal contour shape is varied non-uniformly within a profile tolerance. The blade-row losses, flow capacity, and turning are determined with CFD. The screening results are used to identify the worst-case deviation from the nominal shape. Next, this worst-case airfoil contour deviation is extended to a full 3D blade and the effect on the overall stage performance is evaluated at two tolerance levels.

Screening DOE: Cascade Analysis

At the first stage of the research, the objective was to study the sensitivity of the airfoil contour changes to aerodynamic performance. For this purpose, the nominal blade airfoil contour was modified using a series of piecewise linear offsets. Six points spaced along the fractional surface length of the airfoil defined the offset, as shown conceptually in Figure 1.

The airfoil contour sensitivity study was conducted by means of a 2-Level, 1/4 factorial DOE with 16 runs. The DOE levels for the offset were set to +0.004″ and -0.004″, reflecting the upper end of current

casting process capability. This range was selected to ensure the responses would be discernible. Including the baseline case (nominal geometry), a total of 17 airfoil configurations were examined.

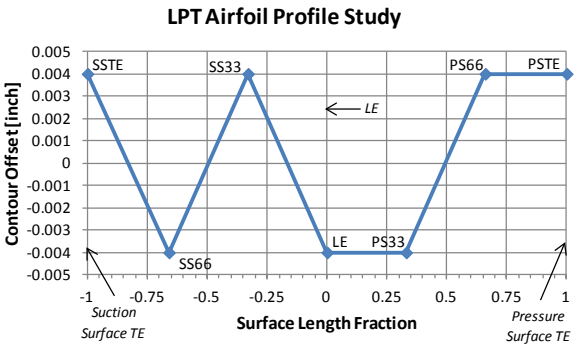

Figure 1. Sample Offset

Figure 2 shows an example of a modified airfoil, overlaid on the nominal contour, and with the six control points located. The offset has been exaggerated to make the deviation obvious. The figure also illustrates the nomenclature used to identify the points in subsequent discussion. The numerical values in the names indicate the percent axial chord where the point is located. Note that SSTE and PSTE refer to the same point and always keep the same offset.

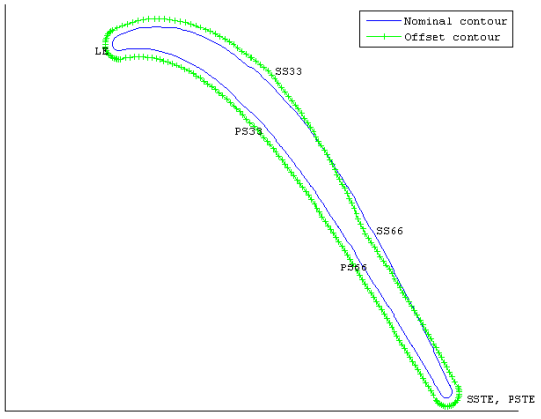

Figure 2. Six control points spaced along the fractional surface length of the airfoil

The baseline airfoil geometry selected for the cascade is the 50% span design section for a typical propulsion LPT blade with a solidity of 1.19. The airfoil contour was "unwrapped" from the conical design surface to a flat (Cartesian) plane. For the cascade analysis, the airfoil was extended as a constant section between the two endwalls. The flowpath featured an annular expansion to simulate the streamtube height change across the original 3D airfoil at 50% span.

The computational domain of the cascade was constructed to model a single passage with an aspect ratio of 2, similar to that shown in Figure 3. A mirror boundary condition at the airfoil mid-span was used so that the domain only extended across half of the cascade, reducing the model size and speeding up the calculations.

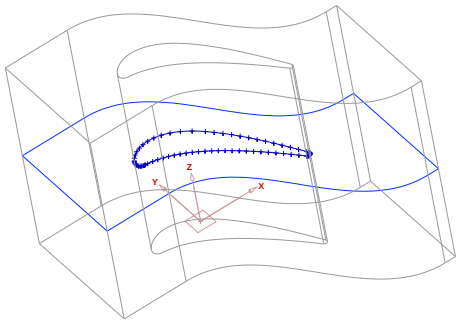

Figure 3. 2D Cascade Geometry

The cascade grid was generated in NUMECA's AutoGrid5. The grid is a structured grid composed of 7 blocks and a total of 306,051 nodes. The grid quality was acceptable, featuring a minimum orthogonality of 54.2 degrees, maximum aspect ratio of 64.1, and maximum expansion ratio of 1.34. The cell width at the airfoil wall was set at .002 inches. The grid nodes on either side of the periodic boundary were matched to minimize interpolation errors. The grid size has been sufficiently refined to adequately resolve the airfoil boundary layer (y+ < 10) around the airfoil.

NUMECA's FINE/Turbo 9.0-2 was utilized to perform the calculations for the 17 cascade cases. The analysis used a steady, viscous, compressible formulation with the SST (Shear Stress Transport) Extended Wall Function turbulence model.

The SST turbulence model is a blended model that combines the two equation turbulence k-ω model with the standard k-ε model.[6] The k-ω model has proven to be superior in numerical stability in the viscous sublayer near solid walls. Near boundary layer edges and in free-shear layers, the model reverts to the k-ε model, written in a k-ω formulation. The SST model modifies the turbulence viscosity function to improve the prediction of separated flows and to avoid the invariably overestimated Reynolds stresses with the k-ω and k-ε models in adverse pressure gradients.

The working fluid is dry air, modeled as a real gas with Cp, k, and μ functions of temperature.

The upper and lower endwalls are modeled with a free-slip condition, since the objective of the analysis is to determine the sensitivity of aerodynamic performance to the 2D airfoil contour. No friction is assumed between fluid and walls in order to avoid the buildup of endwall boundary layers and complications of the associated secondary flows.

All cases were run with boundary conditions representative of the LPT aerodynamic design point. The total pressure, total temperature, and velocity vector cosines were specified at the domain inlet as constant values. The domain exit average static pressure was adjusted to achieve the design point isentropic Mach number of 0.81. The blade-row Reynolds number based on the true chord and the exit flow conditions was 120,600. The turbulence intensity, Tu, was specified at 5%, the level expected in an LPT stage.

Four aerodynamic parameters were selected as the response parameters for the screening DOE: total pressure loss, KE loss coefficient, normalized turning, and corrected flow.

The response parameters extracted from the 17 cascade solutions are summarized in Table 1.

	Pressure Loss	Kinetic Energy Loss	Normalized Turning	Corrected Flow Δ from Baseline
CASE	ΔP'/P'	KE loss coeff	$\Delta\overline{Vy}$	Wcorr
	-	-		%
Baseline	0.0229	0.0485	11.79	0.0
1	0.0245	0.0527	11.95	-1.3
2	0.0259	0.0561	11.84	-0.8
3	0.0218	0.0456	11.90	-0.6
4	0.0216	0.0450	11.64	1.2
5	0.0213	0.0444	11.77	0.3
6	0.0212	0.0440	11.86	-0.3
7	0.0207	0.0428	11.74	0.6
8	0.0224	0.0469	11.68	0.8
9	0.0244	0.0525	11.68	0.5
10	0.0209	0.0433	11.51	2.1
11	0.0216	0.0451	11.55	1.8
12	0.0253	0.0547	12.07	-2.2
13	0.0240	0.0514	11.92	-1.0
14	0.0251	0.0541	11.80	-0.4
15	0.0251	0.0541	11.71	0.2
16	0.0246	0.0529	12.04	-1.9

Table 1. Cascade DOE analysis results

The parameters listed above are defined as follows:

Total Pressure Loss:

$$\frac{\Delta P'}{P'} = \frac{P'_1 - P'_2}{P'_1}$$

KE Loss Coefficient:

$$\bar{e} = 1 - \frac{V_2^2}{V_{2ideal}^2} \qquad \text{where:}$$

$$V_{2ideal}^2 = 2CpT'_1\left[1 - \left(\frac{P_2}{P'_1}\right)^{(\gamma-1)/\gamma}\right]$$

Normalized Turning:

$$\Delta\overline{Vy} = \frac{\Delta Vy}{Vy_1} = \frac{Vy_2 - Vy_1}{Vy_1}$$

The DOE results presented in Table 1 were analyzed with the statistical software Minitab to determine the airfoil contour control points that most affect performance. The statistics were also checked for any strong factor interactions.

A normal probability plot of the effects chart was created for each of the four responses. This chart is used to determine which portions of the fractional airfoil surface length (factors) are significant for the given response. The points that do not fall near the line signal important effects. Important effects are larger and generally further from the fitted line than unimportant effects. Unimportant effects tend to be smaller and centered around zero.

The Pareto chart offers an alternate way of displaying significance. The factors are ranked by magnitude of response and plotted as a bar chart with the most significant at the top.

As an example, Figures 4 and 5 show the normal probability plot and Pareto chart for the total pressure loss. The control points TE, PS66, SS33, and SS66 had a significant effect, in order of importance. The TE had the largest effect, as it controlled the trailing edge thickness, and therefore, the magnitude of the wake losses.

The other three responses were analyzed in a similar way. For the KE loss coefficient, the following factors, in order of importance, were determined to produce a significant response: TE, PS66, SS33, SS66. Note that the order of point sensitivity was the same for both loss coefficients.

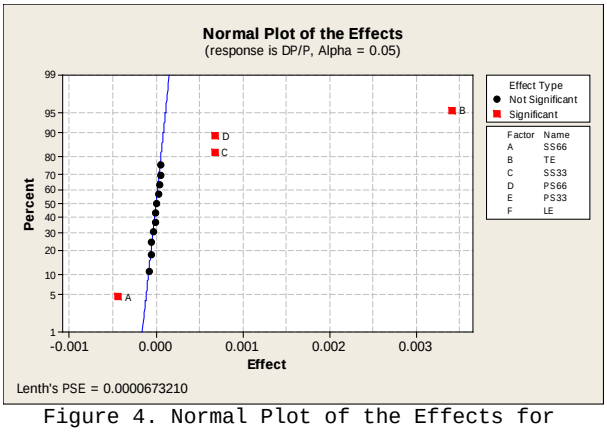

Figure 4. Normal Plot of the Effects for $\Delta P'/P'$

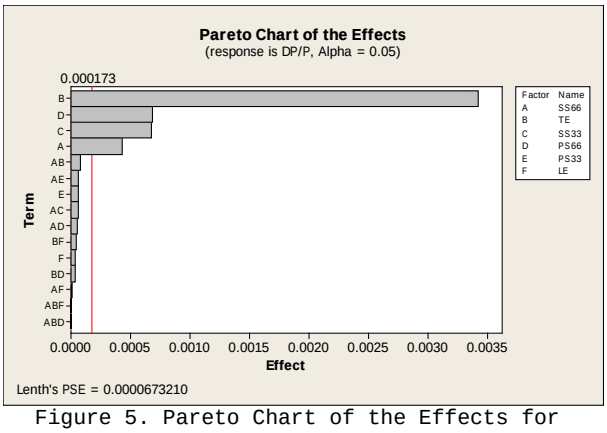

Figure 5. Pareto Chart of the Effects for $\Delta P'/P'$

Additionally, for the normalized turning $\Delta\overline{Vy}$, the following factors were determined to be significant (in order of importance): TE, SS66, PS66, SS33.

For the corrected flow, the significant factors were (in order of importance): TE, SS66, SS33, PS66 and the interaction, SS66*SS33. The first three factors affected the throat opening of the cascade, so this response was not surprising.

From the analysis of variance, it was verified that all the factors listed above (with P values less than .05) were significant for each of the responses. Once the significant factors (TE, PS66, SS33, and SS66) were identified from the cascade DOE analysis, main effects plots for each response

were created to support the selection of control point levels for a worst-case airfoil contour: that which would have the most detrimental impact on the turbine stage performance. Therefore, the worst-case was that which produced the largest losses, the lowest turning, and lowest flow. Figure 6 shows the main effects plot of the significant factors for ΔP′/P′.

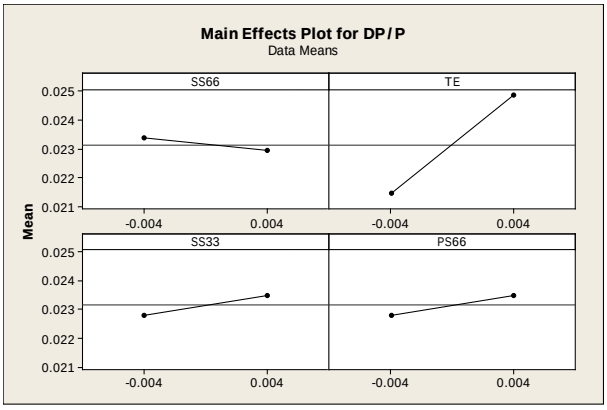

Figure 6. Main Effects Plot for ΔP′/P′ (significant factors)

Additional main effects plots were created for the two factors determined as non-significant for all the selected responses (PS33 and LE). Figure 7 shows the main effects plots for ΔP′/P′ including PS33 and LE.

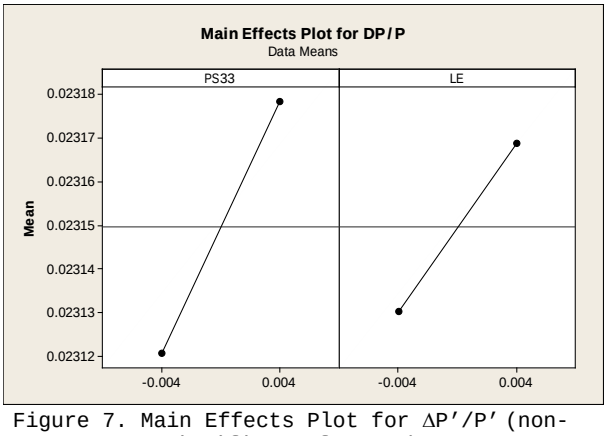

Figure 7. Main Effects Plot for ΔP′/P′ (non-significant factors)

The worst-case levels per factor selected to conduct the 3D stage CFD analysis are shown in Table 2.

Factor	Level	
	Worst-case 1	Worst-case 2
LE	0.003	0.006
TE	0.003	0.006
PS33	0.003	0.006
PS66	0.003	0.006
SS33	0.003	0.006
SS66	-0.003	-0.006

Table 2. Worst-case levels per factor selected to conduct the 3D stage CFD analysis

MBR CFD Analysis: Stage Analysis

To examine the effect of the blade airfoil profile deviations on stage performance, the LPT stage was modeled with FINE/Turbo. Three versions of the LPT stage were examined: nominal blade geometry; worst-case blade with a "tight" airfoil profile of 0.006", representative of the lower end of casting capability; and worst-case blade with a "loose" airfoil profile of 0.012" to ensure a strong impact on the stage performance and capture any second order effects.

The stage grid was generated in AutoGrid5. The computational domain started 1.5 chord lengths upstream of the LPT vane leading edge and extended downstream 1.5 chord lengths beyond the LPT rotor trailing edge.

The stage 3D CFD grid is a structured grid composed of two domains of 7 blocks each: a stationary domain comprising a single vane domain for one blade of the rotor. The vane mean-line solidity was 1.17 and the blade, 1.19.

The grid size was sufficiently refined to adequately resolve the airfoil boundary layer around the airfoil. The grid size was adjusted to target a y+ value <10. Although tip leakage plays an important role on axial turbine efficiency losses, the purpose of this study is to

isolate the effect of airfoil contour geometry on stage losses, therefore tip leakage flows were not modeled.

A total of 1,780,102 nodes was needed for the stage with a minimum orthogonality of 48.7 degrees, maximum aspect ratio of 41.2 and maximum expansion ratio of 1.3. The cell width at the wall is set at .0011 inches. The nodes on the periodic boundaries matched.

Figures 8 to 10 show details of the baseline CFD stage model. For the two worst-case LPT stage models, all blade airfoil design sections were modified with the same contour offset distribution that was selected as a result of the cascade analysis.

The CFD analysis of the stage used a mixing plane to connect the stator (stationary) and rotor (rotating) sub-domains. The SST Extended Wall Function turbulence model was used. The working fluid was viscous, dry air with a typical fuel/air ratio. A real gas model with Cp, k, and μ functions of temperature was used.

The gas properties were supplied to FINE/Turbo in the form of temperature dependent profiles: Cp (Btu/lbm-R), thermal conductivity k (Btu/hr-ft-R) and dynamic viscosity μ (lbm/ft-s).

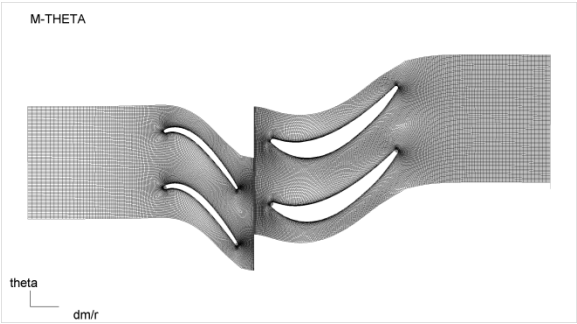

Figure 8. Stage Model B2B Grid

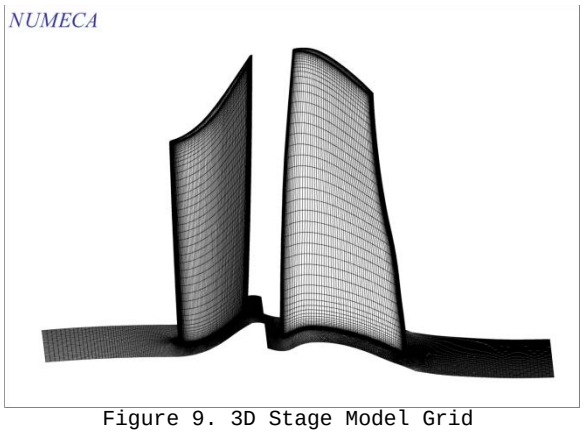

Figure 9. 3D Stage Model Grid

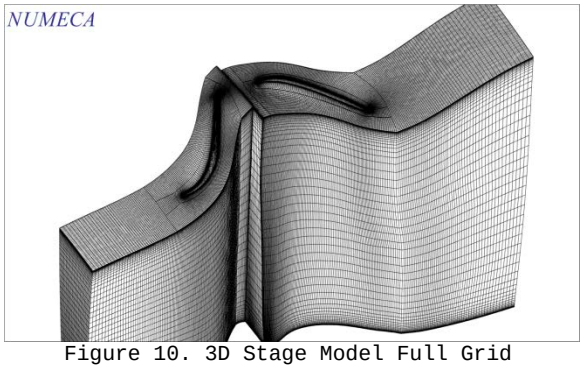

Figure 10. 3D Stage Model Full Grid

All cases were run with boundary conditions representative of the LPT aero design point. The total pressure, total temperature, velocity vector cosines were specified at the domain inlet as airfoil span dependent profiles (Figure 11).

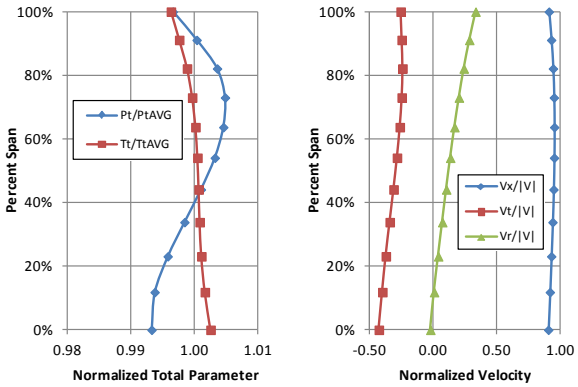

Figure 11. Inlet boundary conditions expressed as span dependent profiles

The domain exit average static pressure was adjusted iteratively to achieve the design LPT pressure ratio total-to-total of 1.772 +/-

.25%. The rotor corrected speed was set to 10,951 rpm. An inlet turbulence intensity of 5% was also specified.

The analyses were run in FINE/Turbo 9.0-2. The solutions were post-processed in CFView to extract the basic aerodynamic quantities. The stage performance calculations were performed with Matlab. The parameters were corrected to standard day temperature and pressure.

The equations used to calculate the stage performance parameters are shown below:

Corrected Flow

$$w_{corr} = \frac{w_1\sqrt{\theta_1}}{\delta_0}$$

Corrected Speed

$$N_{corr}\frac{N}{\sqrt{\theta_1}}$$

Corrected Work

$$\Delta h'_{corr} = \frac{\Delta h'}{\theta_1} = \frac{h'_1 - h'_2}{\theta_1}$$

Corrected Torque

$$\tau_{corr} = \frac{\tau}{\delta_0}$$

Stage efficiency total-to-total

$$\eta = \frac{w_1 \Delta h'_{actual}}{w_1 \Delta h'_{ideal}}$$

The effect of blade profile tolerance on the stage performance parameters is summarized in Table 3.

Case	W_{CORR} [Δ%]	τ_{CORR} [Δ%]	$\Delta h'_{CORR}$ [Δ%]	Δη [%]
Baseline	0.00%	0.00%	0.00%	0.00%
Worst-Case (0.006" Profile Tolerance)	-0.14%	-0.30%	-0.13%	-0.13%
Worst-Case (0.012" Profile Tolerance)	-0.28%	-0.63%	-0.29%	-0.28%

Table 3. Stage Efficiency Parameters

As the allowable profile deviation was increased on the blade, the stage flow and work reduced by similar magnitudes. The drop in torque was about twice as much. As speed was held constant between the cases, the loss in power was also about twice the drop in flow and work. The stage efficiency decreased less than the power because of the offsetting effect of the reduction in the rating flow.

Over the range examined, the effects were linear with tolerance level. From Figure 12, it is seen that the stage efficiency sensitivity to contour profile tolerance is -23.41 points/inch. For corrected flow, the sensitivity is -23.35 %/inch (Figure 13).

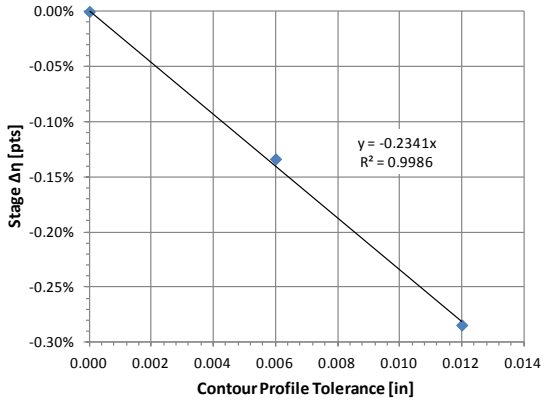

Figure 12. Worst-case blade performance impact –Stage Efficiency-

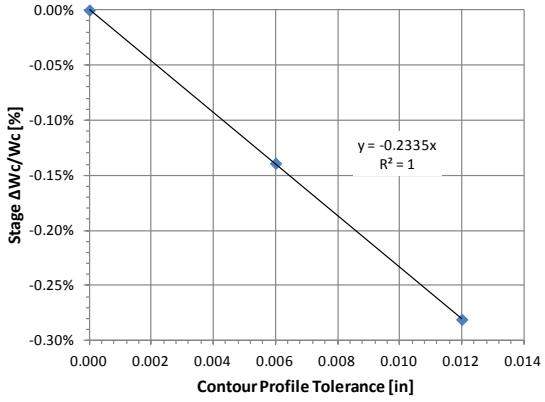

Figure 13. Worst-case blade performance impact –Corrected Flow-

The changes to the blade airfoil contour had very subtle effects on the spanwise distributions. The stage exit Mach number (Figure 14) was essentially unchanged.

The stage pressure ratio (Figure 15) increased near the shroud and decreased near the hub as the airfoil deviation was increased.

The stage work, as represented by the normalized temperature drop (Figure 16) decreased across most of the span. For all three parameters, the magnitude of change was very slight.

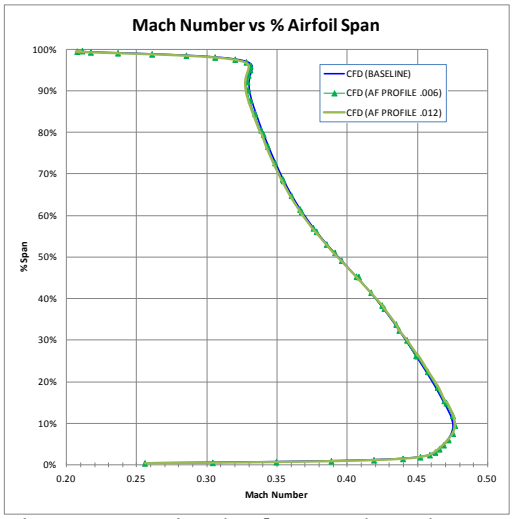

Figure 14. Exit Absolute Mach Number vs % Airfoil Span

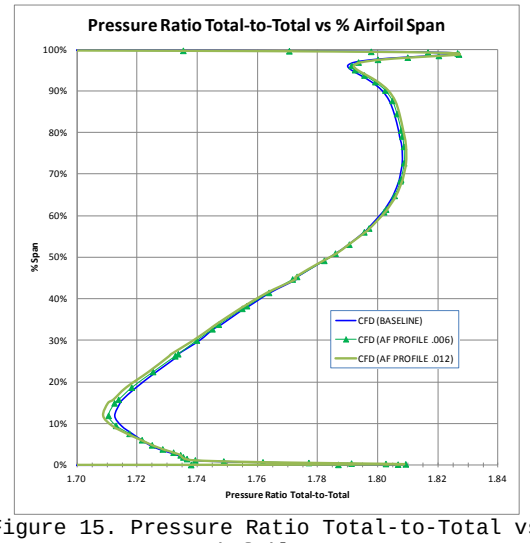

Figure 15. Pressure Ratio Total-to-Total vs % Airfoil Span

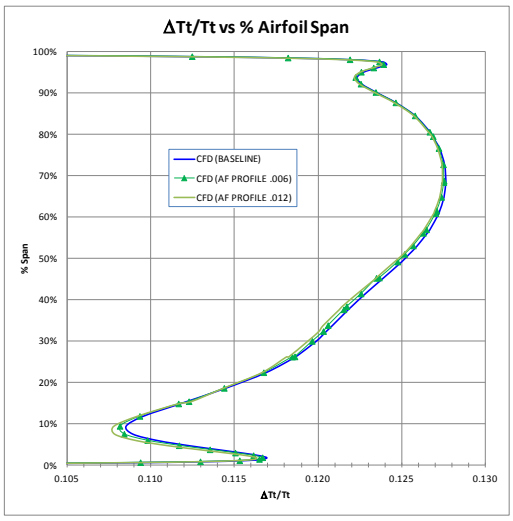

Figure 16. ΔTt/Tt vs % Airfoil Span

Conclusions

In this study an analytical DOE was used to identify a worst-case deviation of a nominal LPT blade airfoil design section (2D) for aerodynamic performance. The resulting offset distribution was applied to a 3D blade at two profile tolerance levels and analyzed as a stage with a nominal vane. The stage performance parameters for the two cases were compared against a baseline case run with the nominal blade geometry.

The airfoil profile tolerance was found to have a non-negligible impact on the turbine stage performance at levels typical of current investment casting process capabilities. When translated to the impact on the engine cycle, the effect on stage efficiency and flow capacity were found to have a small, but still significant impact on engine performance variability.

Striking an appropriate balance between design performance and manufacturability can be assessed with CFD analysis, as was presented here. In the current instance, the results were used to justify a small increase in profile tolerance to improve casting yield.

Finally, the current study greatly simplifies the challenge posed to turbine performance due to manufacturing variation.

Other airfoil tolerances were neglected, such as setting angle, twist, bow, endwall profile, and part-to-part variation of blades within a single rotor. It also was limited to examining variation in one blade-row out of a multi-stage LPT.

More work is required to understand how all the sources of geometric variation contribute to turbine performance both as individual factors and in combination. This knowledge is key to successful management of manufacturing tolerances.

References

[1] Bammert, K., and Sandstede H., “Influences of Manufacturing Tolerances and Surface Roughness of Blades on the Performance of Turbines”, J. Eng. Power. 1976; 98(1): 29-36.

[2] Bammert, K., and Sandstede H., “Measurements Concerning the Influence of Surface Roughness and Profile Changes on the Performance of Gas Turbines”, J. Eng. Power. 1972; 94(3): 207-213.

[3] Bunker, R. S., “The Effects of Manufacturing Tolerances on Gas Turbine Cooling”, Journal of Turbomachinery, Vol. 131, Oct 2009.

[4] Komalkova, D., et al., “Effect of Manufacturing Tolerances on the Turbine Blades”, ASME GTINDIA2014-8253, December 2014.

[5] Montomoli, F., Massini, M., Salvadori, S., “Geometrical uncertainty in turbomachinery: Tip gap and fillet radius”, Computers and Fluids, Vol. 46, n. 1, p 362-368, July 2011.

[6] Menter, F. R., “Two-equation eddy-viscosity turbulence models for engineering applications,” AIAA Journal, v32, n8, pp. 1589-1605, August 1994.